Preplanned Studies

A Three-Year Surveillance Study on Post-pandemic Respiratory Pathogen Ecological Characteristics in Acute Respiratory Infections — Quanzhou City, Fujian Province, China, 2023–2026

Xiaoling Chen[1,2,&]; Changliang Wang[3,4,&]; Weiming Wang[1,2]; Jiajie Huang[1,2]; Manfang Lin[1,2]; Jiangyi Liu[1,2]; Mengjie Yang[1,2]; Caiting Gong[1,2]; Xinlan Huang[1,2]; Jie Zhang[3,4]; Jun Liu[3,4,#]; Youxian Zheng[1,2,#]

Summary

What is already known about this topic?

Post-pandemic circulation of respiratory pathogens has been reshaped, yet evidence from long-term multipathogen surveillance remains scarce.

What is added by this report?

Among 7,029 cases of acute respiratory infection (ARI) in Quanzhou (2023–2026), influenza viruses and SARS-CoV-2 dominated in alternation, while common respiratory viruses co-circulated as multiple subtypes. Viral pathogens tended to be mutually exclusive, whereas bacteria were preferentially codetected. Male sex, older age, pathogen negativity, and certain monoinfections were associated with greater severity; common coinfections were not.

What are the implications for public health practice?

The post-pandemic ARI landscape is a dynamic ecosystem driven jointly by viral interference and bacterial co-colonization, and it calls for sustained multipathogen surveillance.

ABSTRACT

Introduction: Acute respiratory infections (ARIs) are a major global health burden with complex and evolving pathogenic landscapes. Post-pandemic disruptions have altered pathogen circulation, requiring integrated surveillance.

Methods: 7,029 ARI cases from two national sentinel hospitals in Quanzhou (2023–2026) were tested for 30–38 respiratory pathogens by multiplex PCR.

Results: Temporal analyses revealed a dynamic post-pandemic landscape with shifting seasonality, periodic fluctuations, evolving age-specific risks, and inter-/intra-species pathogen heterogeneity. Influenza viruses and SARS-CoV-2 co-dominated with alternating peaks. Respiratory syncytial virus (RSV), human parainfluenza virus (HPIV), seasonal human coronaviruses (HCoVs), and human metapneumovirus (HMPV) exhibited multi-subtype co-circulation. *Mycoplasma pneumoniae* (MP) and adenovirus (AdV) showed short-term atypical surges. A substantial fraction of severe cases remained pathogen-negative. Male sex, advanced age, and monoinfections with RSV, human bocavirus (HBoV), or *Klebsiella pneumoniae* (KP) were independently associated with increased severity. Viral pathogens displayed strong mutual exclusivity, whereas a *Haemophilus influenzae* (HI)/*Streptococcus pneumoniae* (SP)-centered network demonstrated preferential codetection. Common coinfections were not associated with increased severity and, in certain contexts, were linked to reduced severity, potentially reflecting immune priming.

Conclusion: The post-pandemic ARI landscape is a dynamic ecosystem co-driven by viral interference and bacterial co-colonization, requiring integrated multipathogen surveillance.

Acute respiratory infections (ARIs), caused by diverse viral and nonviral pathogens, pose a major global health burden (*1*). Although major respiratory viruses such as influenza viruses, respiratory syncytial virus (RSV), and severe acute respiratory syndrome coronavirus 2 (SARS-CoV-2) are well characterized, most evidence comes from single-pathogen or short-term surveillance, limiting understanding of long-term epidemiology and pathogen interactions. These limitations are particularly relevant in the post-pandemic era when respiratory pathogen circulation is substantially restructured (*2*).

Therefore, a 32-month multiplex PCR-based surveillance study of 7,029 ARI cases was conducted to characterize epidemic dynamics, codetection networks,

Copyright © 2026 by Chinese Center for Disease Control and Prevention

demographic susceptibility, and severity determinants.

Upper respiratory tract specimens were collected weekly from patients with ARI, including influenza-like illness (ILI) and severe acute respiratory infection (SARI), at Quanzhou First Hospital and Quanzhou Children's Hospital, Quanzhou, China, between October 2023 and May 2026. ILI and SARI were defined per World Health Organization (WHO) surveillance case definitions: ILI as a temperature of ≥ 38.0 °C with cough or sore throat in outpatient or emergency patients, whereas SARI as acute fever of ≥ 38.0 °C and cough at admission or within 48 hours with onset within 10 days in inpatients. Eligible consecutive patients were screened until a prespecified monthly quota was reached.

Total nucleic acids were extracted from specimens using a commercial extraction system (Xi'an Tianlong Science and Technology Co., Ltd., Xi'an, China) and amplified with commercial multiplex PCR kits (Beijing Applied Biotech Co., Ltd., Beijing, China): screening used the National Acute Respiratory Infectious Diseases Multipathogen Real-Time PCR Kit (catalog No. D550VYF) and subtyping used version B (catalog No. D404AAYF), both per the manufacturer's instructions (LOD 500 copies/mL). From October 2023 to May 2024, 954 specimens were tested using a 30-target workflow: 14 screening pathogens — influenza A virus (IAV), influenza B virus (IBV), SARS-CoV-2, RSV, adenovirus (AdV), human metapneumovirus (HMPV), human parainfluenza virus (HPIV), seasonal human coronaviruses (HCoVs), human bocavirus (HBoV), human rhinovirus (HRV), enterovirus (EV), *Mycoplasma pneumoniae* (MP), *Chlamydia pneumoniae* (CP), and *Streptococcus pneumoniae* (SP); and 16 reflex subtyping targets — IAV subtypes A(H1N1)pdm09 and A(H3N2), IBV lineage B/Victoria and B/Yamagata, RSV subtypes A and B, HPIV types 1–4, HMPV subtypes A and B, and seasonal HCoV types NL63, OC43, HKU1, and 229E. From June 2024 onward, an expanded 38-pathogen workflow was applied to 6,075 specimens, additionally incorporating *Streptococcus pyogenes* (Group A *Streptococcus*, GAS), *Bordetella pertussis* (BP), *Haemophilus influenzae* (HI), *Legionella pneumophila* (LP), *Klebsiella pneumoniae* (KP), *Aspergillus* species (ASP), *Cryptococcus neoformans* (CN), and *Chlamydia psittaci* (CPS). Pathogens were classified as viral or nonviral (MP, CP, SP, GAS, BP, HI, LP, KP, ASP, CN, and CPS).

Pathogens were clustered using hierarchical clustering of monthly positivity profiles, with pairwise Euclidean distances calculated and agglomerative clustering using ward.D2. Restricted cubic spline (RCS) logistic regression models were used to evaluate the association between age and infection. Pairwise pathogen correlations were assessed using binary presence-absence matrices. "Codetection" (equivalently "coinfection") denotes detection of ≥2 pathogens in one specimen, which may reflect colonization or active infection. RCS and chi-square tests were used to evaluate the associations of age, sex, and infection patterns with severity. Multivariable logistic regression (age- and sex-adjusted) assessed single-pathogen infection effects on severity and the differential risk between coinfections and monoinfections; aORs and 95% *CI*s were reported. Analyses used R 4.5.1 (R Foundation, Vienna, Austria; two-sided $P<0.05$).

From October 2023 to May 2026, 7,029 ARI specimens were collected: 4,627 ILI cases and 2,402 SARI cases (severity: 34.17%), male-to-female ratio 1.26:1.00. Median age was 8 years (1 month–100 years): 14 years (2 months–92 years) for ILI and 6 years (1 month–100 years) for SARI.

Positivity heatmap, temporal line plots, and age-specific RCS curves revealed marked epidemiological heterogeneity among pathogens (Figure 1). Within the high-prevalence cluster, influenza viruses displayed the most pronounced seasonality. IAV peaked in autumn-winter (positivity up to 40%), frequently followed by a delayed B/Victoria subpeak (>20%) in winter-spring of 2023–2024 and 2025–2026, with distinct alternating IAV subtypes. Unlike influenza, SARS-CoV-2 showed no stable seasonality but circulated predominantly in spring-summer, staggered relative to influenza; influenza mainly affected adolescents, whereas SARS-CoV-2 predominated in adults and infants. HRV, HI, and SP showed another high-prevalence pattern, with year-round circulation at relatively high levels (peak >10%) and periodic nonseasonal fluctuations (2–4 months per wave), mainly affecting school-aged children and the elderly. MP and AdV exhibited concurrent elevations restricted to late 2023–early 2024 (peak >15%), then declined, with rapid alteration between influenza subtypes and SARS-CoV-2.

The moderate-prevalence cluster was mainly viral (RSV, HPIVs, seasonal HCoVs, and HMPV), with heterogeneous epidemiological features. RSV predominated in spring-autumn, HMPV in winter-spring, HCoV-NL63 in summer, HCoV-OC43 in autumn-winter, and HPIVs year-round with winter-spring predominance. These circulated at moderate levels (peak approximately 5%) with multiple co-

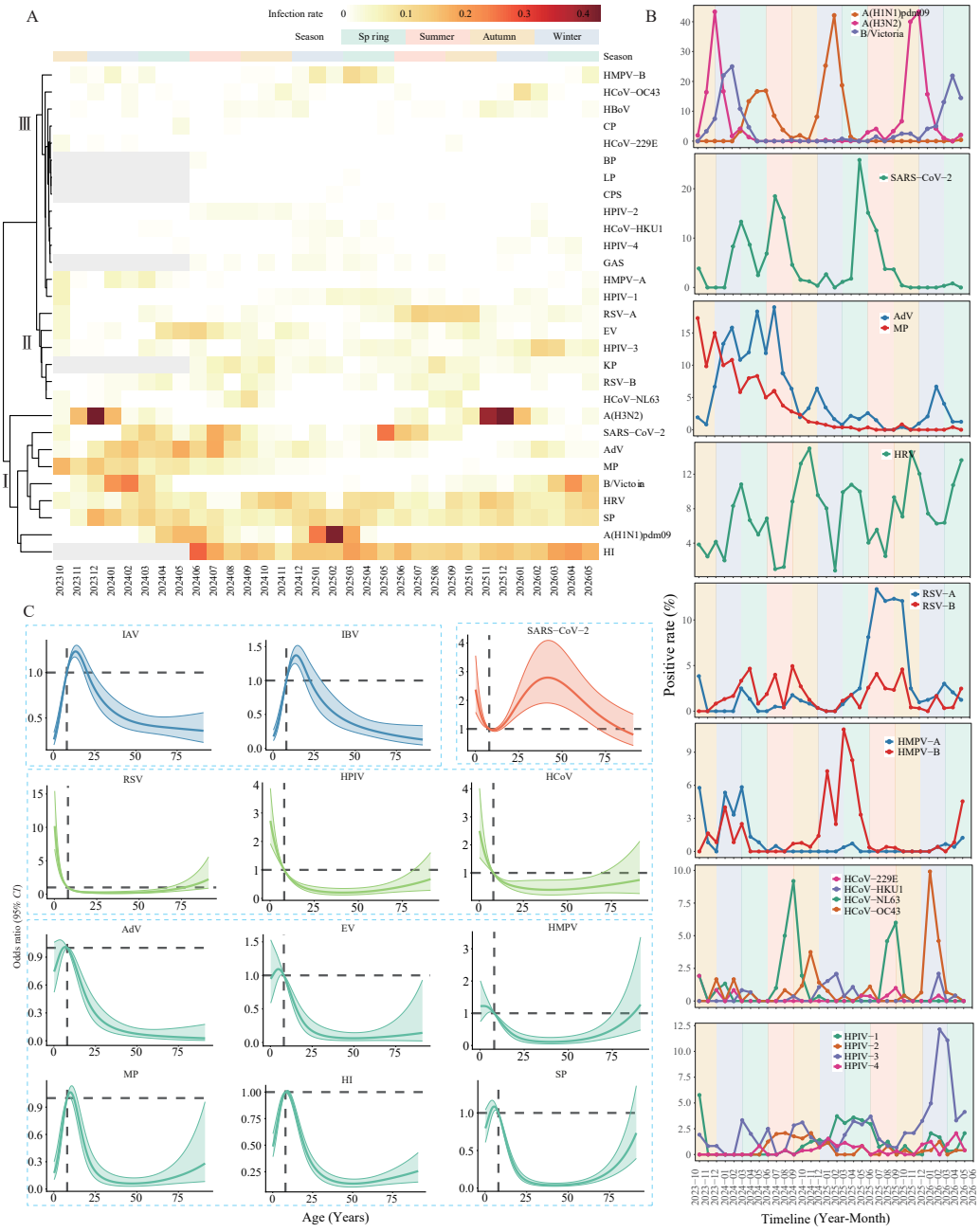


FIGURE 1. Temporal, seasonal, and age-specific patterns of respiratory pathogen infections. (A) The monthly infection rate of each pathogen. (B) The monthly positive rate (%) of predominant pathogens or subtypes from October 2023 to May 2026. (C) Restricted cubic spline (RCS) curves show the adjusted odds ratios (with 95% *CI*s, shaded areas) for pathogen infection across age (0–80 years).

Note: In panel A, the colour scale represents the infection rate, and the top colour bar indicates the season (Spring, Summer, Autumn, Winter). Pathogens are grouped into clusters I–III by hierarchical clustering. In panel B, the background colours indicate seasons. In panel C, the dashed horizontal line marks an odds ratio of 1.0. Curves of the same colour indicate pathogens with similar age-specific patterns. For all pathogens shown, both *P* overall and *P* non-linearity were < 0.05.

Abbreviation: HMPV=human metapneumovirus; HCoVs=human coronaviruses; HBoV=human bocavirus; CP=*Chlamydia pneumoniae*; HCoV=seasonal human coronavirus; BP=*Bordetella pertussis*; LP=*Legionella pneumophila*; CPS=*Chlamydia psittaci*; HPIV=human parainfluenza virus; GAS=Group A *Streptococcus*; EV=enterovirus; KP=*Klebsiella pneumoniae*; A(H3N2)=influenza A(H3N2); SARS-CoV-2=severe acute respiratory syndrome coronavirus 2; AdV=adenovirus; MP=*Mycoplasma pneumoniae*; B/Victoria=influenza B/Victoria lineage; HRV=human rhinovirus; SP=*Streptococcus pneumoniae*; A(H1N1)pdm09=influenza A(H1N1)pdm09; HI=*Haemophilus influenzae*; IAV=influenza A virus; IBV=influenza B virus; *CI*=confidence interval.

circulating subtypes, although dominant subtypes (e.g., RSV-A, HCoV-NL63/OC43, HPIV-3, and HMPV-B) occasionally exceeded 10%. RSV, HPIVs, and seasonal HCoVs exhibited L-shaped age-specific positivity, highest at the youngest and oldest ages, especially among infants; HMPV additionally showed elderly susceptibility. Remaining pathogens circulated at low levels.

Viral pathogens predominated in monoinfections, whereas nonviral pathogens were more frequent in coinfections. Among 6,075 participants tested for 38 respiratory pathogens, 46.47% (2,823/6,075) had no pathogen detected; 36.43% (2,213/6,075) had monoinfection (27.79% viral, 8.64% nonviral); and 17.10% (1,039/6,075) had coinfection (2.01% viral, 1.00% nonviral, 14.11% viral-nonviral).

Correlation analysis showed strong positive correlations between HI and SP, and between each of these bacteria and most viruses; by contrast, viruses, particularly influenza viruses and SARS-CoV-2, displayed strong mutual exclusivity. Moderate positive correlations were noted for MP+EV, GAS+SP, and HBoV+HPIV (Figure 2A).

The top coinfecting pathogens were HI (64.87%, 674/1,039), SP (37.44%, 389/1,039), HRV (23.97%, 249/1,039), and AdV (10.11%, 105/1,039), which occupied the hub positions and linked to numerous other pathogens (Figure 2B). Common viral-nonviral combinations were IAV+HI (n=145), HRV+HI (n=123), and IAV+SP (n=94). The most frequent nonviral coinfection was HI+SP (n=177), whereas IAV+HRV (n=31) was the most common viral coinfection.

RCS curves showed that individuals aged ≥50 years had an elevated risk of developing severe disease. Chi-square tests demonstrated severity differed significantly by sex and infection pattern, with a higher severity proportion in males than in females (39.7% *vs.* 27.4%). Notably, pathogen-negative (no pathogen detected) cases had the highest severity proportion (40.2%), whereas viral-nonviral coinfections had the lowest (21.4%).

In a multivariable logistic regression adjusted for age and sex (reference: pathogen-negative cases) (Figure 3A), RSV, HBoV, and KP monoinfections were independently associated with increased odds of severity; these findings require caution because comorbidities were unavailable. In contrast, HI, SARS-CoV-2, and influenza monoinfections were associated with more ILI cases, with no significant severity-related associations for remaining pathogens.

Compared with corresponding monoinfections (Figure 3B), most coinfections showed no increased severity. Only SARS-CoV-2/AdV *vs.* SARS-CoV-2 monoinfection and MP/HI *vs.* HI monoinfection were significantly associated with higher severity. Several HI, SP, or HRV coinfections with viruses appeared protective.

DISCUSSION

Influenza viruses and SARS-CoV-2 remained predominant, with epidemic peaks far exceeding those of other pathogens. Multiple regional reports (*3*–*4*) indicate intensified post-COVID-19 influenza activity with a bimodal winter-summer pattern. In this study, both viruses co-dominated; influenza likewise showed a bimodal pattern with subtype alternations, alongside atypical MP and AdV co-circulation early post-pandemic. These changes are widely attributed to the "immunity gap" arising from altered population immunity, behavioral patterns, viral interactions, and healthcare practices post-pandemic (*2*,*5*). However, these surges cannot be directly attributed to the immunity gap, given the lack of pre-2023 baseline data. Unlike influenza, SARS-CoV-2 has not yet established a stable seasonal pattern or consistent peak magnitude, although it shows staggered circulation relative to influenza (*6*). In this study, these two viruses also differed in susceptible populations; influenza predominantly affected adolescents, whereas SARS-CoV-2 was more frequent in adults and infants. Notably, HI, SP, and HRV exhibited another distinct high-detection pattern, characterized by year-round periodic circulation and high coinfection rates.

The moderate-prevalence cluster comprised RSV, HPIVs, seasonal HCoVs, and HMPV, with frequent subtype co-circulation and occasional predominance of RSV-A, HCoV-NL63/OC43, HPIV-3, and HMPV-B. In Quanzhou, their seasonal distributions were heterogeneous, concordant with others (*7*): RSV showed extended spring-autumn activity, HMPV retained winter-spring predominance, HCoV-NL63 peaked in summer, HCoV-OC43 in autumn-winter, and HPIVs circulated year-round with winter-spring predominance. Although these pathogens shared similar susceptible populations at both age extremes, RSV displayed a particularly stronger association with severe disease; however, this was adjusted only for age and sex, without comorbidity data. Dominant subtypes in Quanzhou differed from those reported in other Chinese regions concurrently (*8*), highlighting regional

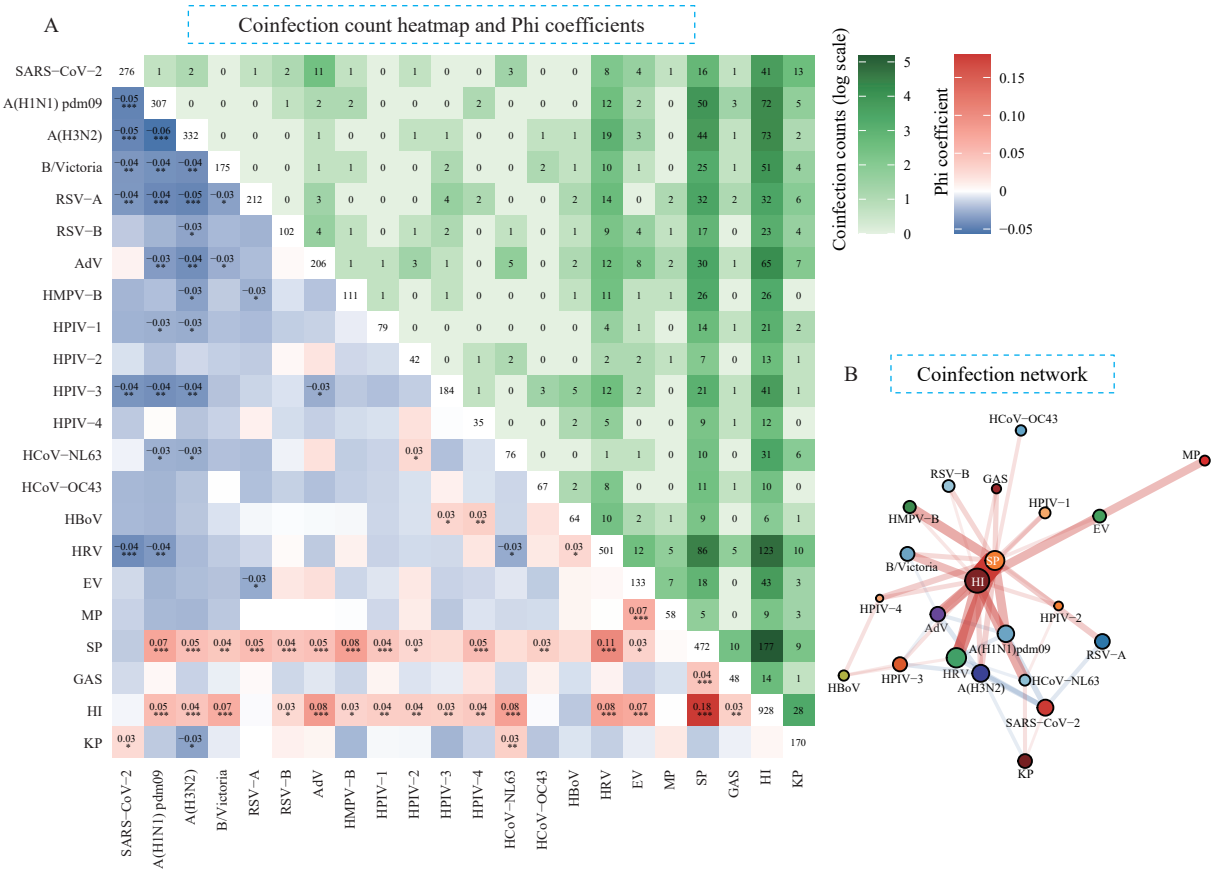


FIGURE 2. Coinfection patterns among respiratory pathogens. (A) The coinfection counts heatmap and the Phi coefficients. (B) The coinfection network.

Note: In panel A, the upper triangle shows coinfection counts, and the lower triangle shows *Phi* coefficients; the colour scales are shown on the right. In panel B, the nodes represent individual pathogens, and edges indicate coinfections, with node size and edge width proportional to coinfection frequency. Only pathogens with detected coinfections are shown.

Abbreviation: SARS-CoV-2=severe acute respiratory syndrome coronavirus 2; A(H1N1)pdm09=influenza A(H1N1)pdm09; A(H3N2)=influenza A(H3N2); B/Victoria=influenza B/Victoria lineage; RSV=respiratory syncytial virus; AdV=adenovirus; HMPV=human metapneumovirus; HPIV=human parainfluenza virus; HCoV=seasonal human coronavirus; HBoV=human bocavirus; HRV=human rhinovirus; EV=enterovirus; MP=*Mycoplasma pneumoniae*; SP=*Streptococcus pneumoniae*; GAS=Group A *Streptococcus*; HI=*Haemophilus influenzae*; KP=*Klebsiella pneumoniae*.

* *P*<0.05, ** *P*<0.01, *** *P*<0.001.

heterogeneity. These findings depict a dynamic post-pandemic ARI landscape with overlapping seasonality, pathogen reshuffling, and shifting age-specific risks.

Significant mutual exclusivity has been observed among viral pathogens, particularly between influenza viruses and SARS-CoV-2. Such viral interference, potentially mediated by interferon-driven innate immunity (*9*–*10*), may contribute to asynchronous circulation and partly explain the staggered epidemic dynamics. However, this exclusivity was not evident between viral and bacterial pathogens, particularly HI and SP. HI and SP occupied central nodes within the coinfection network, exhibiting strong positive correlations and frequent codetection with diverse viruses, underscoring bacterial roles in airway co-colonization (*11*).

Advanced age and male sex were identified as risk factors for severe disease. After adjustment, specific coinfection analyses showed no evidence that the top coinfecting pathogens (e.g., HI, SP, and HRV) exacerbated severity; in some cases, they appeared protective (*12*). Because colonization cannot be distinguished from active infection and comorbidity data are unavailable, these associations may reflect a healthy carrier effect, temporal ambiguity, or residual confounding rather than a true biological effect. Although viral-bacterial coinfections are traditionally thought to synergistically increase severity, accumulating evidence indicates certain bacteria can antagonize viral infections. Manna et al. (*13*) reported

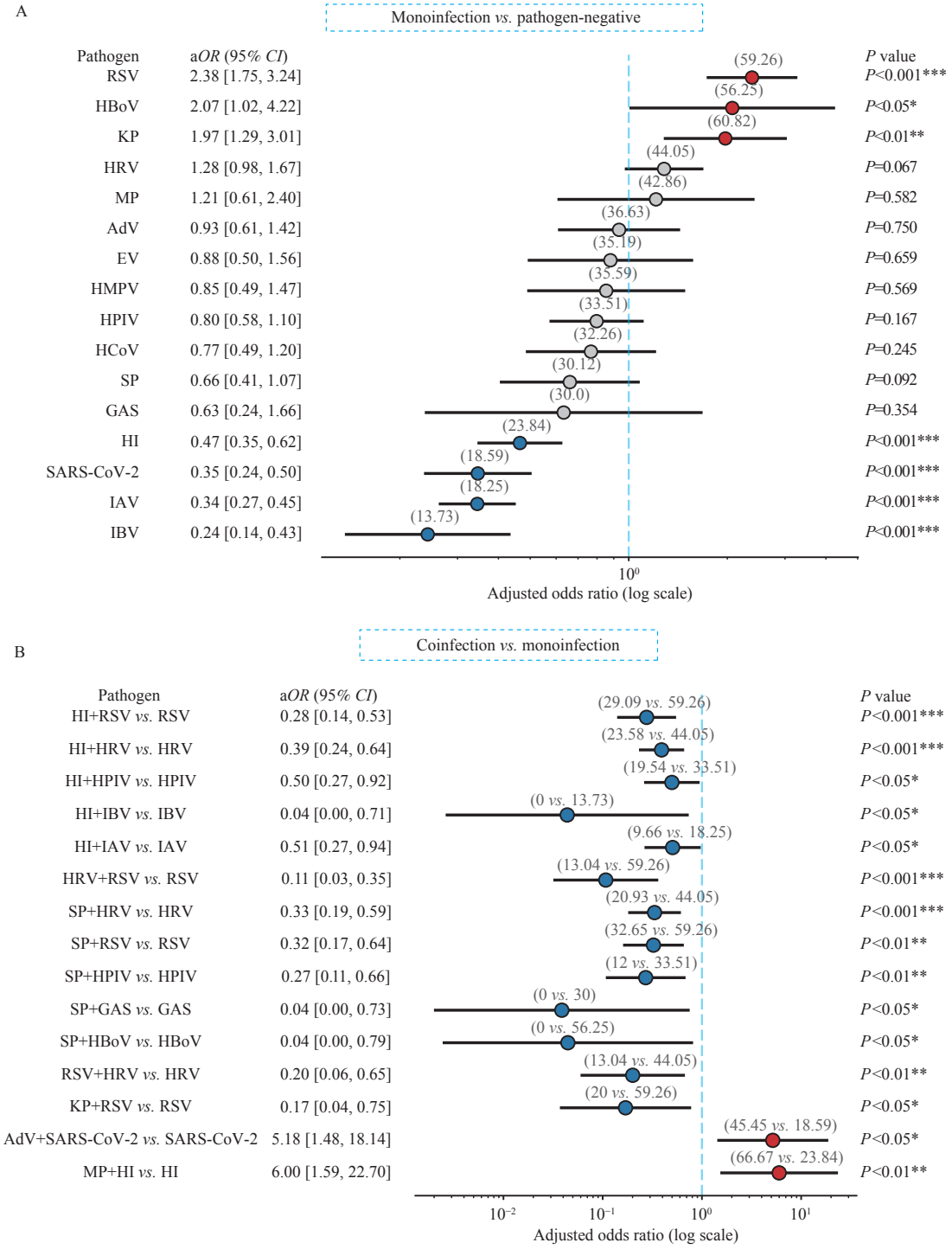


FIGURE 3. Adjusted odds ratios for severe outcomes in monoinfection and coinfection analyses. (A) Monoinfection *vs.* pathogen-negative cases. (B) Coinfection *vs.* monoinfection.

Note: Points represent a*OR*s; horizontal lines indicate 95% *CI*s; the dashed vertical line marks a*OR*=1. Blue points indicate a*OR*<1, red points a*OR*>1, and grey points *CI*s crossing 1. Values are plotted on a logarithmic scale. In (A), values in parentheses above each point are the corresponding severity rates. In (B), only pathogens with *P*<0.05 are shown.

Abbreviation: RSV=respiratory syncytial virus; HBoV=human bocavirus; KP=*Klebsiella pneumoniae*; HRV=human rhinovirus; MP=*Mycoplasma pneumoniae*; AdV=adenovirus; EV=enterovirus; HMPV=human metapneumovirus; HPIV=human parainfluenza virus; HCoVs=seasonal human coronaviruses; SP=*Streptococcus pneumoniae*; GAS=Group A *Streptococcus*; HI=*Haemophilus influenzae*; SARS-CoV-2=severe acute respiratory syndrome coronavirus 2; IAV=influenza A virus; IBV=influenza B virus; aOR=adjusted odds ratio; *CI*=confidence interval.

* *P*<0.05, ** *P*<0.01, *** *P*<0.001.

that live SP colonization accelerates clearance of multiple respiratory viruses. Hou et al. (*14*) demonstrated that preexisting SP colonization enhances interferon signaling, antiviral responses, and CD8+ T cell responses, suggesting bacterial colonization primes host immunity via trained innate immunity. Nevertheless, several uncommon combinations showed strong severity associations, underscoring potential synergies when mutually exclusive pathogens are co-detected. Collectively, clinical consequences of coinfections are not uniform but shaped by complex ecological interactions, depending on specific pathogen combinations and temporal context.

This study has limitations. Nucleic acid testing cannot distinguish active infections from carriers or shedding. Notably, pathogen-negative cases exhibited the highest severity proportion, potentially reflecting limited assay sensitivity (e.g., for novel or fungal pathogens) or noninfectious etiologies. This highlights the need for diversified detection, including lower respiratory tract sampling and broad-range sequencing. Limited case numbers for some combinations may have biased severity analyses, and residual confounding from comorbidities, vaccination status, and healthcare-seeking behavior was not adjusted for. Future studies should incorporate longitudinal sampling and host immune profiling.

In summary, this large ultra-multiplex cohort provides a robust framework for investigating respiratory pathogen ecology. These findings underscore the importance of comprehensive multiplex surveillance for understanding post-pandemic respiratory pathogen ecology and may inform adaptive prevention strategies.

Conflicts of interest: No conflicts of interest.

Ethical statement: Approved by the Ethics Committee of Quanzhou Center for Disease Control and Prevention.

Funding: Supported by the Quanzhou Science and Technology Development Funds (2025QZNY039). J.L. is supported by the National Natural Science Foundation of China Young Scientists Fund (A) (82525060).

doi: 10.46234/ccdcw2026.220

[#] Corresponding authors: Youxian Zheng, zyx7405@fjmu.edu.cn; Jun Liu, liu_jun01@gzlab.ac.cn.

[1] The Affiliated Quanzhou Center for Disease Control and Prevention of Fujian Medical University, Quanzhou City, Fujian Province, China; [2] Quanzhou Center for Disease Control and Prevention (Quanzhou Health Supervision Institute), Quanzhou City, Fujian Province, China; [3] Strategic Pandemic Preparedness Action and Research Centre (SPARC), Guangzhou National Laboratory, Guangzhou City, Guangdong Province, China; [4] State Key Laboratory of Respiratory Disease, National Clinical Research Centre for Respiratory Disease, National Centre for Respiratory Medicine, Guangzhou Institute of Respiratory Health, The First Affiliated Hospital of Guangzhou Medical University, Guangzhou Medical University, Guangzhou City, Guangdong Province, China.

[&] Joint first authors.

Copyright © 2026 by Chinese Center for Disease Control and Prevention & Chinese Academy of Preventive Medicine. All content is distributed under a Creative Commons Attribution Non Commercial License 4.0 (CC BY-NC).

Submitted: August 07, 2026
Accepted: October 24, 2026
Issued: October 30, 2026

REFERENCES

1. GBD 2023 Lower Respiratory Infections and Antimicrobial Resistance Collaborators. Global burden of lower respiratory infections and aetiologies, 1990-2023: a systematic analysis for the Global Burden of Disease Study 2023. Lancet Infect Dis 2026;26(4):343 – 61. https://doi.org/10.1016/S1473-3099(25)00689-9.
2. Liu WJ, Liu SL. A tale of two cities: from influenza HxNy to SARS-CoV-z. China CDC Wkly 2021;3(49):1052 – 6. https://doi.org/10.46234/ccdcw2021.256.
3. Chen W, Wang HB, Ten XL, Fu M, Lin ML, Xu XP, et al. Impact of COVID-19 control measures on influenza positivity among patients with acute respiratory infections, 2018-2023: an interrupted time series analysis. BMC Infect Dis 2025;25(1):925. https://doi.org/10.1186/s12879-025-11279-6.
4. Chen C, Liu HM, Liu JY, Chen PF, Lu HZ. Changing epidemiology of respiratory pathogens since 2020: Shenzhen case study and global perspectives. Drug Discov Ther 2025;19(5):277 – 84. https://doi.org/10.5582/ddt.2025.01108.
5. Liu J, Wong G, Li H, Yang Y, Cao YX, Li YF, et al. Biosafety and immunology: an interdisciplinary field for health priority. Biosaf Health 2024;6(5):310 – 8. https://doi.org/10.1016/j.bsheal.2024.07.005.
6. Zhang JN, Guo YY, Sang JY, Tian JM, Lyu C, Hu YC, et al. Population immunology: building a population immune barrier for pandemic preparedness. Chin J Microbiol Immunol 2026;47(7):557 – 67. https://doi.org/10.3760/cma.j.cn112309-20260514-00188.
7. Rios-Guzman E, Simons LM, Dean TJ, Agnes F, Pawlowski A, Alisoltanidehkordi A, et al. Deviations in RSV epidemiological patterns and population structures in the United States following the COVID-19 pandemic. Nat Commun 2024;15(1):3374. https://doi.org/10.1038/s41467-024-47757-9.
8. Du H, Li J, Wen HY, Gu ZX, Chang YF, Rong WW, et al. Respiratory pathogen profiles of patients — Beijing municipality, China, November 2023–April 2024. China CDC Wkly 2025;7(4):113 – 20. https://doi.org/10.46234/ccdcw2025.018.
9. Deol P, Miura TA. Respiratory viral coinfections: interactions, mechanisms and clinical implications. Nat Rev Microbiol 2025;23(12):757 – 70. https://doi.org/10.1038/s41579-025-01225-3.
10. Cheemarla NR, Watkins TA, Mihaylova VT, Foxman EF. Viral Interference during influenza A–SARS-CoV-2 coinfection of the human airway epithelium and reversal by oseltamivir. J Infect Dis 2024;229(5):1430 – 4. https://doi.org/10.1093/infdis/jiad402.
11. Lewnard JA, Huppert A, Givon-Lavi N, Pettigrew MM, Regev-Yochay G, Dagan R, et al. Density, serotype diversity, and fitness of *Streptococcus pneumoniae* in upper respiratory tract cocolonization with nontypeable *Haemophilus influenzae*. J Infect Dis 2016;214(9):1411 – 20. https://doi.org/10.1093/infdis/jiw381.
12. Liu WJ, Zou RR, Hu YF, Zhao M, Quan CS, Tan SG, et al. Clinical,

immunological and bacteriological characteristics of H7N9 patients nosocomially co-infected by *Acinetobacter baumannii*: a case control study. BMC Infect Dis 2018;18(1):664. https://doi.org/10.1186/s12879-018-3447-4.

13. Manna S, McAuley J, Jacobson J, Nguyen CD, Ullah A, Sebina I, et al. Synergism and antagonism of bacterial-viral coinfection in the upper respiratory tract. mSphere 2022;7(1):e00984 – 21. https://doi.org/10.1128/msphere.00984-21.
14. Hou H, McAuley J, Maluenda A, Mulholland K, Phipps S, Wijburg O, et al. Nasopharyngeal colonisation by Streptococcus pneumoniae enhances host anti-viral responses to respiratory virus infection. bioRxiv [Preprint]. 2025 Dec 11 [cited 2026 Jun 28]. Available from: https://doi.org/10.64898/2025.12.10.693560.